Magnetoconvection in a plane layer rotating about the horizontal axis: The effect of anisotropic diffusivities

Tomáš ŠOLTIS[1], Jozef BRESTENSKÝ[2]

[1] Geophysical Institute of the Slovak Academy of Sciences,
  Dúbravská cesta 9, 845 28 Bratislava, Slovak Republic; e-mail: geoftoso@savba.sk

[2] Deparment of Astronomy, Physics of the Earth and Meteorology,
  Faculty of Mathematics, Physics and Informatics, Comenius University
  Mlynská dolina F-1, 842 48 Bratislava, Slovak Republic, e-mail: brestensky@fmph.uniba.sk

Abstract: A linear stability analysis of convection arising in a horizontal plane layer rotating about the horizontal axis and permeated by a homogeneous horizontal magnetic field perpendicular to the rotation axis is performed. Resulting horizontal convective rolls are inclined to the magnetic field at an angle dependent on the dimensionless numbers − the Elsasser, Ekman and Roberts numbers, and moreover on the anisotropy parameter, the ratio of horizontal and vertical diffusion coefficients (which are the viscosity and thermal diffusivity; magnetic diffusivity is considered isotropic).

Two types of anisotropies, SA and BM, are considered and compared with the isotropic case of diffusion coefficients. In the stratification anisotropy, SA, of the Sa and So types, diffusivities in the horizontal directions are, respectively, smaller and greater than the vertical ones. In the BM anisotropy (*Braginsky and Meytlis, 1990*), the diffusivities in the directions of rotation axis and magnetic field – in the horizontal directions are greater than in vertical direction, thus identically as in So type anisotropy. Results of this $\mathcal{H}$ case, the model with the horizontal rotation axis, are compared with the $\mathcal{V}$ case of a similar model with the vertical rotation axis. The modes of instabilities are much more sensitive to viscosity and various anisotropies in the $\mathcal{H}$ case than in the $\mathcal{V}$ case.

Results indicate that the effects of anisotropic diffusivities on the Earth's core magnetoconvection and geodynamo processes should be studied more thoroughly in simpler models than is usually done.

Key words: anisotropic diffusion coefficients, rotating magnetoconvection, horizontal rotation axis, Earth's core, geomagnetic field

1. Introduction

In the geodynamo problem the basic MAC dynamic balance corresponding to the *M*agnetic, *A*rchimedean and *C*oriolis forces can be sensitively

affected by diffusion processes variously weakening the individual forces. Thus magnetic and thermal diffusion weaken the M and A forces, respectively, while viscosity weakens the C force, which can lead to a new balance of the forces with the possibility of instabilities completly different from those in the diffusionless case. In recent years geodynamo computational simulations (see e.g. *Fearn and Roberts, 2007*) have paid close attention to the dependence on various Prandtl numbers representing ratios of different diffusion coefficients or characteristic times of diffusions. Despite the fact that some diffusion coefficients are unrealistically high, e.g. viscosity, due to numerical limitations, results of the simulations are of great heuristic significance (*Fearn and Roberts, 2007; Gubbins and Herrero-Bervera, 2007*). Experiments, better approaching some parameter values of the Earth's core conditions, are also significant in the sense of geodynamo problem (*Gailitis et al., 2002; Aurnou, 2007*). Therefore, the study of more complicated anisotropic diffusion coefficients is useful.

It is believed, due to the highly developed convection in the Earth's core, that the core is in a turbulent state (*Braginsky and Meytlis, 1990; Fearn and Roberts, 2007; Schubert, 2007*) and turbulent[1] transport of momentum and heat is more effective when compared with molecular transport. Turbulent transport of the magnetic field is not as effective, because the molecular magnetic diffusivity, η, based on high electrical conductivity of the Earth's outer core, used in geodynamo models is sufficient to explain basic features of the geomagnetic field. Thus, the turbulent magnetic diffusivity, η_T, is less than or, at most, comparable to η, while the turbulent diffusion coefficients, ν_T and κ_T, are much greater than their molecular counterparts, ν and κ. The effective diffusivities, well represented by ν_T, κ_T and η (or $\eta + \eta_T$), are supposed to be of the same order of magnitude (*Fearn and Roberts, 2007*). But due to the effect of the Lorentz and Coriolis forces the turbulence is highly anisotropic, since turbulent eddies are deformed into a shape elongated in the direction parallel to the magnetic field and the

---

[1] *Braginsky and Meytlis (1990)* focused attention on a source of turbulence different from classical turbulence due the buoyancy in unstably stratified fluids. In this so-called convectively generated turbulence, eddies arise on all space scales, but their persistence is strongly limited. Contrary to classical turbulence, generated by shear stresses, in which the energy is transported from larger to smaller eddies, here due to the buoyancy the eddies of all possible sizes arise. They live independently with no mutual effects among the eddies of other sizes.

rotation axis. Since turbulent small-scale eddies are diffusers of momentum and heat, the effective viscosity and thermal diffusion is also anisostropic. *Braginsky and Meytlis (1990)* showed that the momentum and heat should diffuse parallel to the rotation axis and in the direction of the prevailing magnetic field much more effectively than in the direction perpendicular to both. Anisotropy of magnetic diffusivity is not considered in this paper, because it is possible that the turbulence affects the effective magnetic diffusivity only negligibly. Due to the fact that turbulent eddies are too small to be resolved with the current generation of computers, parameterization of subgrid scales is usually used. Firstly, it was a trick with hyperdiffusivities (see e.g. *Fearn and Roberts, 2007*) which overcame the numerical problems in geodynamo simulations. However, the hyperdiffusivities with no physical background are a rough analogue of anisotropy in the sense that viscosity is greater in horizontal directions (in a spherical surface) than in the vertical (radial) direction, which roughly resembles the anisotropy of diffusion coefficients in oceanic surface waters, in which values in horizontal directions exceed those in the vertical direction by up to several orders of magnitude (see e.g. *Cushman-Roisin, 1994*). Of course, this stratification anisotropy, is different from the results of *Braginsky and Meytlis (1990)*.

Therefore, in *Šoltis and Brestenský (2010)* two different types of anisotropy were introduced: stratification anisotropy, SA, analogous to hyperdiffusivity and BM anisotropy based on *Braginsky and Meytlis (1990)*. SA is determined by the single vector gravity $\boldsymbol{g}$ and BM anisotropy by the pair of vectors $\boldsymbol{\Omega}_0$ and $\boldsymbol{B}$ (angular velocity and magnetic field). Both anisotropies in *Šoltis and Brestenský (2010)* were, possibly, of the simplest form in which viscosity and thermal diffusion are expressed by a diagonal tensor (of order two represented as a 3×3 array) with only two different values of its three components; e.g. $\nu_{xx} = \nu_{yy} \neq \nu_{zz}$, $\kappa_{xx} = \kappa_{yy} \neq \kappa_{zz}$ for the SA anisotropy with preserved horizontal isotropy. A simple measure of anisotropy, convenient for both SA and BM ones, was defined by the ratios $\alpha = \nu_{xx}/\nu_{zz} = \kappa_{xx}/\kappa_{zz}$ and was called the anisotropy parameter; see the last column in Table 1. It is used also here; see the last of (7).

The SA anisotropy, determined by the vertical direction, is studied in this paper. If the diffusion coefficients in the horizontal directions are smaller than in the vertical direction, $\alpha < 1$, then SA anisotropy is called the stratification anisotropy of the atmospheric type and is labeled Sa. Contrary,

Table 1. Comparison of properties of setups in approaches to anisotropic diffusivities in *Donald and Roberts (2004)*, *Ivers and Phillips (2007–2012)*, *Šoltis and Brestenský (2010)* and in this paper; convection = rotating convection and rotating magnetoconvection in *Ivers and Phillips (2007–2012)* and *Šoltis and Brestenský (2010)*, respectively. In both $\mathcal{V}$ and $\mathcal{H}$ cases with the rotation axis in vertical and horizontal directions, respectively, two definitions (8) of the Rayleigh number are applied.

paper(s) model properties	*Donald and Roberts (2004)*	*Ivers and Phillips (2007–2012)*	*Šoltis and Brestenský (2010)* + this paper $\mathcal{V} + \mathcal{H}$ case
problem	dynamo	convection	convection
geometry	sphere	sphere	plane layer
coordinates	cylindrical, $s\varphi z$	cylindrical, $s\varphi z$	Cartesian, xyz
z axis	rotation axis	rotation axis	vertical $\parallel \boldsymbol{g}$
anisotropy parameter	$\beta = \dfrac{1-\alpha}{1+\alpha}$	$\zeta = \dfrac{1}{\alpha} - 1$	$\alpha = \dfrac{\kappa_{xx}}{\kappa_{zz}} \left(= \dfrac{\kappa_{ss}}{\kappa_{zz}} \right)$
Rayleigh number $\propto$	$1/(\kappa_{zz} + \kappa_{ss})$	$1/(\kappa_{zz} + 2\kappa_{ss})$	$1/\kappa_{zz}$ and $1/\kappa_{xx}$
anisotropic diffusivities	$\boldsymbol{\kappa}$	$\boldsymbol{\kappa}$	$\boldsymbol{\kappa}, \boldsymbol{\nu}$
isotropic diffusivities	ν, η	ν, η	η
magnetic field	$B_\varphi(s, z)\, \hat{\boldsymbol{\varphi}}$	no field	$B_M \hat{\mathbf{y}}, B_M = const$

if $\alpha > 1$, then we speak of stratification anisotropy of the oceanic type, labeled *So* (*Šoltis and Brestenský, 2010*). Here the *So* anisotropy can be also considered as BM one. Due to the orientations of the rotation axis and the magnetic field in horizontal directions the definition of the BM anisotropy and of the SA one for $\alpha > 0$ is now formally equal. The clear distinction of SA and BM anisotropies was possible in *Šoltis and Brestenský (2010)*, because of the vertical rotation axis. Henceforth, we shortly distinguish the $\mathcal{H}$ and $\mathcal{V}$ cases with the horizontal and vertical rotation axis studied here and in *Šoltis and Brestenský (2010)*, respectively. In both cases, $\mathcal{H}$ and $\mathcal{V}$, a homogeneous horizontal magnetic field is considered.

One might wonder whether the effects of various anisotropic diffusion coefficients on the geodynamo or at least magnetoconvection are known. There is, for instance, a pilot study of an example of the anisotropy influence on operation of the intermediate dynamo in *Donald and Roberts (2004)*. The

comprehensive attempt to include the effects of anisotropic thermal diffusion in geodynamo models is described by Phillips and Ivers (see e.g. *Phillips and Ivers, 2003*). The influence of this anisotropy on the rotating magnetoconvection is presently not sufficiently known, but there are attempts in *Brestenský et al. (2005)*, *Šoltis and Brestenský (2010)*, *Ivers and Phillips (2007–2012)* and also here. The magnetoconvection studied here is of a large scale for a majority of geophysically realistic input parameters, while small scale instabilities[2] responsible for this anisotropy are not the central interest in our study.

The basis of the present $\mathcal{H}$ case study is the approximation in *Roberts and Jones (2000)*, $\nu \gg \kappa \sim \eta$, i.e. comparable coefficients of thermal and magnetic diffusion, κ and η, respectively, but significantly larger viscosity, ν. It ignores inertial oscillations as well as torsional oscillations, which gives us the chance to focus attention mainly on the MAC dynamics neglecting also the nonlinear inertial force $\boldsymbol{u} \cdot \nabla \boldsymbol{u}$ here and in *Brestenský and Šoltis (2014)*, *Roberts and Jones (2000)*, *Šoltis and Brestenský (2010)*, which is typical in modeling the Earth's core turbulence (*Fearn and Roberts, 2007; Gubbins and Herrero-Bervera, 2007; Schubert, 2007*).

Our approach to the study of the anisotropy of diffusion coefficients (see e.g. *Šoltis and Brestenský (2010)* or this paper) is in principle different from the currently prevailing ones. For instance, in *Donald and Roberts (2004)* and *Phillips and Ivers (2003)*, the influence of anisotropic diffusion coefficients on the dynamo is studied, while in *Matsushima et al. (1999)*, analogically like in *Braginsky and Meytlis (1990)*, properties of turbulent diffusion coefficients are derived from a model of rotating magnetoconvection with prescribed isotropic diffusion coefficients. In *Braginsky and Meytlis (1990)*, the linear stability analysis is not concentrated on marginal instabilities but on those, which have the fastest exponential growth rate of amplitudes. In *Braginsky and Meytlis (1990)* and *Matsushima et al. (1999)* the conditions for the onset of convection are, respectively, studied in the whole space or in a box on the surface of a sphere, thus in a geometry different from our plane layer. In the latter case (*Matsushima et al., 1999*), dependence on the latitude is also studied.

---

[2] We hope that not only the advanced turbulence, but even any regular flow of the smaller space and time scales can be parameterized to acquire "turbulent" diffusion coefficients as input parameters to study the onset of instabilities of the greater scales.

It is not only the geometry (the horizontal plane layer) which differs from the above mentioned simplifications or from the spherical geometry attempts (*Phillips and Ivers, 2003*) or our emphasis on the marginal modes that make our approach so different. It is that we suppose a priori anisotropic diffusion coefficients as in *Donald and Roberts (2004)* in the case of the dynamo or in *Ivers and Phillips (2007–2012)* in the case of rotating convection or in *Šoltis and Brestenský (2010)*, *Brestenský et al. (2005)* in the cases of magnetoconvection, and then we study conditions for the onset of convection. The above mentioned studies (*Braginsky and Meytlis, 1990; Matsushima et al., 1999*) or many other rotating magnetoconvection studies contemplate only isotropic input diffusivities based on molecular values. In our approach the anisotropic diffusivities would be a result of some parameterization of turbulent small scale flows, but determined by the dynamic MAC balance. Then our choice of effective diffusivities corresponding to the turbulent anisotropic diffusivities is analogous to the usually used turbulent isotropic diffusivities in various dynamo or magnetoconvection models (*Fearn and Roberts, 2007*), in which the turbulent flow – the source of the parameterization – is not considered.

One of the interesting results in the $\mathcal{V}$ case (*Šoltis and Brestenský, 2010*) is the sensitivity of the marginal convection to the SA anisotropy. For example, So anisotropy increases and Sa decreases the horizontal dimension of the steady rolls. But, the opposite is true for some non-stationary modes. However, the convection is more sensitive to the BM anisotropy, because the horizontal isotropy of the diffusion coefficients is broken in that case. In the SA case it is not broken.

The main inspiration and motivation for the paper are in *Donald and Roberts (2004)* and *Ivers and Phillips (2007–2012)*, see Table 1. The paper *Donald and Roberts (2004)* inspired us to study magnetoconvection models with input anisotropic diffusion coefficients. In a rotating convection model in a sphere, *Ivers and Phillips (2007–2012)* confirmed our results for a horizontal plane layer rotating about the vertical axis, presented in conferences, e.g. SEDI 2004 and 2006 in GaPa and Prague (but see *Šoltis and Brestenský, 2010*; *Brestenský et al., 2005*). This confirmation for properties of arising instabilities in our case $\mathcal{V}$ (*Šoltis and Brestenský, 2010*) was only partial. The monotonicity of the critical Rayleigh number vs the SA anisotropy cases contradicted in *Ivers and Phillips (2007–2012)* and *Šoltis and Brestenský*

(2010) in the sense that in our case the Sa anisotropy decreased the critical Rayleigh number, R_c, while in *Ivers and Phillips (2007–2012)* it increased R_c, and oppositely the So anisotropy decreased and increased R_c in *Šoltis and Brestenský (2010)* and *Ivers and Phillips (2007–2012)*, respectively. We have supposed that the main reason for this contradiction is in various geometries, i.e. the spherical in *Ivers and Phillips (2007–2012)* and plane layer geometry in *Šoltis and Brestenský (2010)*. Therefore, it has motivated us to solve the magnetoconvection model in the $\mathcal{H}$ case of a plane layer. However, it seems (see Table 1) geometry is not the only factor that determines the differences among *Donald and Roberts (2004)*, *Ivers and Phillips (2007–2012)* and *Šoltis and Brestenský (2010)*. It can also be the definition of the Rayleigh number, as indicated in this paper.

We partially follow the $\mathcal{H}$ case models in *Eltayeb (1972, 1975)*, *Eltayeb and Rahman (2013)* and *Kurt et al. (2004)*. In the rotating horizontal plane layer permeated by a homogeneous horizontal magnetic field we consider the horizontal rotation axis perpendicular to the magnetic field and we use a linear stability analysis with marginal instabilities in the form of horizontal rolls. We compare the $\mathcal{H}$ and $\mathcal{V}$ cases by the approach in *Roberts and Jones (2000)* in which unlike *Eltayeb (1972)*, attention is focused on regime diagrams determining regions of preference of various modes of convection for different input parameters, e.g. Λ, E_z and q_z defined in (7). This comparison of the $\mathcal{H}$ and $\mathcal{V}$ cases is made only for the SA anisotropy, similar to how it is done in *Brestenský and Šoltis (2014)* for the isotropic case, $\alpha = 1$.

Our attention to the $\mathcal{H}$ case and the comparison of both cases, $\mathcal{H}$ and $\mathcal{V}$, is not motivated only by various delicate dynamics and balance of the basic forces, M, A and C in various rotating conditions. The main motivation in the study is the role of various diffusive processes, which can compete with one another (*Šimkanin et al., 2003*). This competition is very complex, in particular if the anisotropic diffusion coefficients are considered (*Ivers and Phillips, 2007–2012; Šoltis and Brestenský, 2010; Brestenský et al., 2005; Šoltis, 2010*).

The structure of the paper is as follows. The setting of the model is given in Section 2. The basic equations are discussed and the dispersion relation derived using a linear stability analysis is in Section 3. Further analytical methods of solution and solutions for steady and non-stationary convection are contained in Section 4. Numerical results and comparison with analyt-

ical derivations are discussed in Section 5. The most important results are summarized and the paper concluded in Section 6.

2. Model

The basic state with the imposed homogeneous magnetic field in the y-direction and with the rotation axis in the x-direction is considered in the $\mathcal{H}$ case. This configuration considers gravity in the vertical z-direction with a rough analogy to the equatorial regions of the Earth's core (*Brestenský and Šoltis, 2014*). In this configuration of the basic state, all the directions determining the three basic forces (M, A, C) are mutually perpendicular.

That is why it is important to investigate how anisotropy of diffusion coefficients influences the balance of these forces, how conditions for formation of the convection change, and how the space and time structure of the convection itself are changed. The anisotropy parameter α is defined as in *Šoltis and Brestenský (2010)*; see Table 1 and the last of (7).

3. Basic equations

The $\mathcal{H}$ case model is described with the following fundamental equations in the linearized and dimensionless form

$$R_o\frac{\partial \boldsymbol{u}}{\partial t} + \hat{\mathbf{x}} \times \boldsymbol{u} = -\nabla p + \varLambda(\nabla \times \boldsymbol{b}) \times \hat{\mathbf{y}} + R\,\vartheta\,\hat{\mathbf{z}} + E_z\nabla_\alpha^2\boldsymbol{u}\,, \tag{1}$$

$$\frac{\partial \boldsymbol{b}}{\partial t} = \nabla \times (\boldsymbol{u} \times \hat{\mathbf{y}}) + \nabla^2\boldsymbol{b}\,, \tag{2}$$

$$\frac{1}{q_z}\frac{\partial \vartheta}{\partial t} = \hat{\mathbf{z}} \cdot \boldsymbol{u} + \nabla_\alpha^2\vartheta\,, \tag{3}$$

$$\nabla \cdot \boldsymbol{u} = 0, \quad \nabla \cdot \boldsymbol{b} = 0\,. \tag{4}$$

In comparison to the $\mathcal{V}$ case, the only change is in the Navier-Stokes equation in its' Coriolis term $\hat{\mathbf{x}} \times \boldsymbol{u}$ (here the horizontal rotation axis in the x-direction is considered).
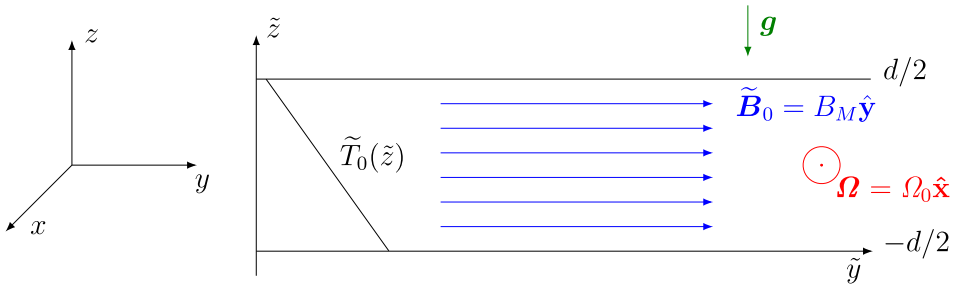
Fig. 1. Model of the rotating magnetoconvection with the basic homogeneous horizontal magnetic field in an infinite horizontal unstably stratified layer with the vertical temperature profile $\widetilde{T}_0(\tilde{z})$ and rotating about a horizontal axis perpendicular to the magnetic field. Here in the $\mathcal{H}$ case the arrow of the vector $\boldsymbol{\Omega}$ is directed towards the reader, while in the $\mathcal{V}$ case $\boldsymbol{\Omega}$ is antiparallel to $\boldsymbol{g}$.

The BM and SA anisotropies in the $\mathcal{H}$ case have a formally equivalent mathematical formulation, that is why the anisotropic Laplacian in the terms $E_z\nabla_\alpha^2\boldsymbol{u}$ and $\nabla_\alpha^2\vartheta$ in (1) and (3) now has the single form

$$\nabla_\alpha^2 = [(1-\alpha)\partial_{zz}^2 + \alpha\nabla^2] \tag{5}$$

and not two distinct forms as in the $\mathcal{V}$ case; see (8-10) in *Šoltis and Brestenský (2010)*.

If we set the anisotropy parameter α equal to one, then we get, from the anisotropy versions of these diffusion terms, the commonly used forms $E\nabla^2\boldsymbol{u}$ and $\nabla^2\vartheta$. In the equations (1–4) dimensionless variables are used and they are defined in the usual way

$$z \to dz, \quad t \to \frac{d^2}{\eta}t, \quad \boldsymbol{u} \to \frac{\eta}{d}\boldsymbol{u}, \quad p \to 2\Omega_0\eta\rho_0 p, \quad \boldsymbol{b} \to B_M\boldsymbol{b}, \quad \vartheta \to \frac{\eta\Delta T}{\kappa_{zz}}\vartheta, \tag{6}$$

where d and d^2/η are the typical length and characteristic time (magnetic diffusion time). So the dimensionless numbers appearing in the equations (1–3) are defined as in the case $\mathcal{V}$ (*Šoltis and Brestenský, 2010*), i.e.

$$R_o = \frac{\eta}{2\Omega_0 d^2}, \quad \Lambda = \frac{B_M^2}{2\Omega_0\rho_0\mu\eta}, \quad E_z = \frac{\nu_{zz}}{2\Omega_0 d^2}, \quad q_z = \frac{\kappa_{zz}}{\eta}, \quad \alpha = \frac{\nu_{xx}}{\nu_{zz}} = \frac{\kappa_{xx}}{\kappa_{zz}}, \tag{7}$$

where we have Rossby, Elsasser, Ekman, and Roberts numbers and an anisotropy parameter. ρ_0, p, μ and η are density, pressure (with a contribution from the centrifugal force), magnetic permeability and diffusivity,

respectively. Further, two Rayleigh numbers,

$$R = \frac{\alpha_T g \Delta T d}{2\Omega_0 \kappa_{zz}} \quad \text{and} \quad R_{eff} = \frac{\alpha_T g \Delta T d}{2\Omega_0 \kappa_{xx}} = \frac{R}{\alpha}, \tag{8}$$

are introduced, where the modified Rayleigh number R is the same as in *Šoltis and Brestenský (2010)* and where α_T is the thermal expansion coefficient. One can wonder, whether R or the effective Rayleigh number R_{eff} is more convenient for understanding the marginal convection onset. It is discussed in subsection 5.3, but this paper deals mainly with the Rayleigh number defined by the first of (8).

We focus our attention on instabilities of MAC wave type as in *Brestenský and Šoltis (2014)*, *Eltayeb (1972)*, *Šoltis and Brestenský (2010)*, and therefore we consider the limit $\nu \gg \kappa \sim \eta$, due to which the Rossby number R_o in (1) is negligible. In the next procedure we will use the fact that disturbances of the magnetic field $\boldsymbol{b}$ and the velocity $\boldsymbol{u}$ can be divided into toroidal and poloidal parts in the form

$$\boldsymbol{u} = a^{-2} \left[\nabla \times (\nabla \times w\hat{\mathbf{z}}) + \nabla \times \omega\hat{\mathbf{z}} \right], \quad \boldsymbol{b} = a^{-2} \left[\nabla \times (\nabla \times b\hat{\mathbf{z}}) + \nabla \times j\hat{\mathbf{z}} \right], \tag{9}$$

since $\boldsymbol{b}$ and $\boldsymbol{u}$ are solenoidal. Disturbances (w, ω, b, j and ϑ) have the form

$$f(x, y, z, t) = \Re e \left[F(z) \exp(ilx + imy) \exp(\lambda t) \right], \tag{10}$$

where l and m are the horizontal components of the wave vector, $a = \sqrt{l^2 + m^2}$ is the horizontal wave number (18) and λ is the complex frequency ($\lambda = i\sigma$). Next, the curl operator and the double curl operator are applied to the Navier-Stokes equation. The curl operator is also applied to the induction equation and, after substitution of the disturbances (w, ω, b, j, and ϑ) into these equations ($\nabla \times$NS, $\nabla \times \nabla \times$NS, IE, $\nabla \times$IE)[3] and the heat conduction equation, and considering only the $\hat{\mathbf{z}}$ components, the following set of ordinary differential equations for the unknown functions $F(z) = W(z)$, $\Omega(z)$, $B(z)$, $J(z)$ and $\Theta(z)$ is obtained

$$[E_z \mathcal{D}_\alpha - R_o \lambda] \, \Omega + ilW + im\Lambda J = 0, \tag{11}$$

$$(D^2 - a^2) [E_z \mathcal{D}_\alpha - R_o \lambda] \, W - il\Omega + im\Lambda (D^2 - a^2)B = a^2 R\Theta, \tag{12}$$

---

[3] NS and IE are the Navier-Stokes and the induction equation, respectively.

$$(D^2 - a^2 - \lambda)J + im\Omega = 0, \tag{13}$$

$$(D^2 - a^2 - \lambda)B + imW = 0, \tag{14}$$

$$(\mathcal{D}_\alpha - \lambda/q_z)\Theta + W = 0, \tag{15}$$

where the operator D means d/dz and $\mathcal{D}_\alpha = D^2 - \alpha a^2$. In the next formulas and computations the Rossby number (see R_o in (11, 12)) is already considered to be zero. When comparing this equation system (11−15) to the similar system for the $\mathcal{V}$ case, we can see that the difference is only in two terms, ilW and $-il\Omega$, in the equations (11) and (12), respectively. Corresponding terms in the $\mathcal{V}$ case are DW and $-D\Omega$. Now, the operator $\mathcal{D}_\alpha$ has the single form $\mathcal{D}_\alpha = D^2 - \alpha l^2 - \alpha m^2$, unlike the $\mathcal{V}$ case, where it has two different forms depending on the type of anisotropy, SA or BM. But now $\mathcal{D}_\alpha$ reflects only the horizontal isotropy, which was violated in the $\mathcal{V}$ case for the BM anisotropy. We consider the boundary conditions at $z = -1/2, 1/2$ for the mechanically free and thermally and electrically perfectly conductive boundaries

$$W = D^2W = D\Omega = \Theta = B = DJ = 0, \tag{16}$$

which are the simplest ones in the $\mathcal{V}$ case with solutions W, Θ, $B \propto \cos \pi z$, and Ω, $J \propto \sin \pi z$ (*Šoltis and Brestenský, 2010*). Here in the $\mathcal{H}$ case we suppose that the trigonometric solutions, exact in the $\mathcal{V}$ case, are good approximations for mainstream solutions outside of boundary layers. The arguing for it, and the solutions of $F(z)$ in the isotropic case convenient also for the boundary layers can be found in *Eltayeb and Rahman (2013)* and in *Brestenský and Šoltis (2014)*, too.

Applying the same algebraic procedures as in the $\mathcal{V}$ case and using our limit $\nu/\eta \to \infty$, we derive a very similar dispersion equation

$$Ra^2 \frac{q_z(K^2 + \lambda)}{(q_z K_\alpha^2 + \lambda)} = \frac{K^2[E_z(K^2 + \lambda)K_\alpha^2 + m^2\Lambda]^2 + l^2(K^2 + \lambda)^2}{E_z(K^2 + \lambda)K_\alpha^2 + m^2\Lambda}, \tag{17}$$

where $K^2 = \pi^2 + a^2$ and $K_\alpha^2 = \pi^2 + \alpha a^2$. The difference, compared to the $\mathcal{V}$ case is in the last term in the numerator of the right hand side, which has changed in the following way

$$\pi^2(K^2 + \lambda)^2 \to l^2(K^2 + \lambda)^2.$$

The main task of our investigation is to find the preferred modes, while, from the very beginning, we will concentrate on the marginal modes, for which $\Re e(\lambda) = 0$. The first step is to find, for all l and m, modes in the form of stationary convection with $\Im m(\lambda) = 0$ or overstability with $\Im m(\lambda) = \sigma \neq 0$. We will label the Rayleigh number of stationary convection R^s and the Rayleigh number for the overstability R^o. The next step is to find, for both convection types (for the given E_z, Λ and q_z), a critical mode, i.e. l and m, such that $R^s(l,m)$ and $R^o(l,m)$ are smallest. The last step is to denote, which of R^s_c and R^o_c is less and, therefore, preferred.

4. Modes of stationary and non-stationary convection in the form of rolls

Convection in the form of stationary and nonstationary horizontal rolls investigated here in the case $\mathcal{H}$ as well as in the case $\mathcal{V}$ (*Roberts and Jones, 2000; Šoltis and Brestenský, 2010*), is clearly described by the two components, l and m, of the horizontal wave vector. The pair, l and m (see (10)), can be substituted by another pair,

$$a = (l^2 + m^2)^{1/2} \quad \text{and} \quad \gamma = \tan^{-1}(m/l), \tag{18}$$

the magnitude of the horizontal wave vector, and the angle between the rolls and the basic magnetic field in the y-direction (see Fig. 2), respectively. The vector (l, m) determines the orientation of convective rolls (the rolls are perpendicular to the vector) and in the case of nonstationary convection, this vector determines also the direction of propagation of the wave (*Brestenský and Šoltis, 2014*). If $l = 0$, then we speak of cross rolls, since they are oriented perpendicularly to the basic magnetic field. The rolls with $m = 0$ are called parallel. If both wave numbers are nonzero, then we speak of oblique rolls. Both the Coriolis and Lorentz forces try to tilt the convection rolls into the direction of the rotation axis or the direction of the magnetic field, respectively. The cross rolls can be viewed also as the rolls for which the Coriolis force has played the dominant role, because the rolls are tilted exactly parallel to the rotation axis (i.e. perpendicularly to the magnetic field). There is the result that motions in the rolls do not feel the Coriolis force. For the parallel rolls the Lorentz force has played the dominant
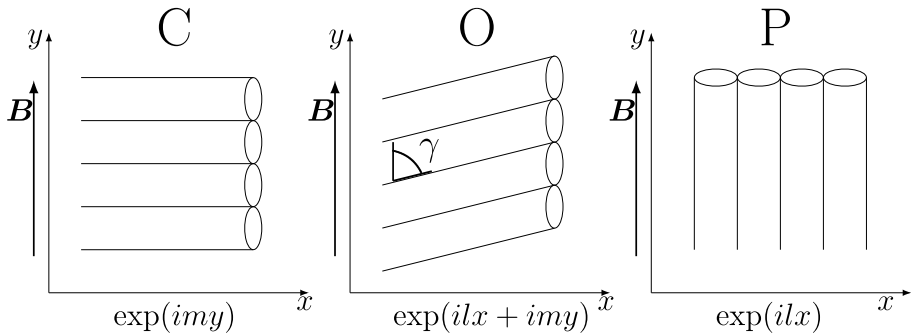
Fig. 2. Different orientations of convective horizontal rolls. $\gamma = \tan^{-1}(m/l)$ is the angle between the axis of the rolls and the magnetic field $\boldsymbol{B}$. Three sets, {SC and OC}, {SO, OC$'$ and OO} and {P} of stationary or non-stationary modes, correspond to the C, O and P rolls, respectively, in the $\mathcal{H}$ case. In the $\mathcal{V}$ case the OC$'$ modes do not arise.

influence with rolls tilted parallel to the magnetic field, i.e. the motions in the rolls finally do not feel the Lorentz force. In the case of oblique rolls the Lorentz and Coriolis forces are in a balance in which the convective rolls are oriented at a certain angle towards the magnetic field and rotation axis. By combination of the three possible orientations of rolls with stationary (steady) and nonstationary (overstable) convection, 5 (+1) different modes of convection are defined. We will name them, using labeling and names according to Roberts and Jones (*Jones and Roberts, 2000; Roberts and Jones, 2000*), the P, SC, SO, OC and OO modes[4]. P modes are never overstable, similarly to the $\mathcal{V}$ case, because λ in (17) is a real number. The OC$'$ modes are special OO modes, the rolls of which are almost perpendicular to the magnetic field. The SO, OO, OC' and OC modes are named by *Eltayeb (1975)* the steady oblique, old oblique, new oblique (or "the modified oblique mode") and "the magnetic roll" mode, respectively. In *Eltayeb and Rahman (2013)* the names of modes are adapted to their dynamic background, "the modified magnetic mode" (= OC') and "the aligned magnetic modes", steady (SAM = SC) or overstable (OAM = OC). The stationary (P, SO and SC) and nonstationary (OO and OC) modes occur in both com-

---

[4] The labeling for regimes of convection of P, SC, SO, OC and OO modes or rolls comes from the names parallel, steady cross, steady oblique, overstable cross and overstable oblique, respectively.

pared cases, $\mathcal{V}$ and $\mathcal{H}$, while the nonstationary OC$'$ modes only in the $\mathcal{H}$ case for all investigated values of the anisotropy parameter α.

The dispersion equation (17) is for the most common initial layout of the problem. Two extreme cases can occur in the minimization of the Rayleigh number $R = R(l, m)$, the P modes or the C modes, where $m = 0$ or $l = 0$, respectively. The zero value of one component is one condition in determination of the minimum R. The second condition is given by the derivative $\partial R / \partial a^2$ or $\partial R / \partial \tilde{a}$. Henceforth, we use

$$\tilde{a} = a^2/\pi^2 = \tilde{l} + \tilde{m}, \quad \text{with} \quad \tilde{l} = l^2/\pi^2, \quad \tilde{m} = m^2/\pi^2. \tag{19}$$

The role of C modes (SC and OC modes in comparison with other modes) is more significant in the $\mathcal{H}$ case than in the $\mathcal{V}$ case. Further, the OC$'$ modes are more similar to the C modes because of their almost colinearity with the rotation axis. The $\mathcal{H}$ case can be regarded as an approximation for the equatorial regions of the Earth's core and therefore the C and OC$'$ modes roughly correspond to rotating convection in spherical geometry[5] or in the Busse annulus. Minimizing for rolls of the general tilt with $l \neq 0$ and $m \neq 0$ needs to compute one more partial derivative; e.g. $\partial R / \partial \tilde{l} = 0$ and $\partial R / \partial \tilde{m} = 0$.

4.1. Stationary modes

We can see immediately from (17) that stationary modes with $\lambda = 0$ are independent of q_z. Due to (11, 12) the stationary convection is also independent of the Rossby number R_o. Thus, the approximation $R_o = 0$ does not influence the properties of the SC, SO and P modes, because they are the same for all values of q_z and R_o (or R_o/E). This fact gives the chance to compare the results in this section with the linear stability study of the model in *Kurt et al. (2004)*. The difference between the two models is in the approximating limiting cases, $q_z \to 0$ (i.e. $\kappa \ll \eta$) and $E/R_o \to 0$ (i.e. $\nu \ll \eta$), in *Kurt et al. (2004)* and $\nu \gg \kappa$ and $\nu \gg \eta$ in this paper, respectively. Therefore, the resulting properties of stationary convection are

---

[5] Many properties of axially-aligned columns in spherical geometry and the C and OC$'$ rolls in our $\mathcal{H}$ case are similar. One of the reasons for some non-similarities can be unboundedness of the plane layer with infinite length of the rolls contrary to the finite volume of the sphere or spherical shell. A comprehensive analysis of modes in the spherical geometry is e.g. in *Gubbins and Herrero-Bervera (2007)*.

the same in both models, because the stationary modes are not sensitive to the Prandtl numbers, q_z and E/R_o, i.e. the Roberts and magnetic Prandtl number. By the way, the SC, SO and P modes are named the axial, oblique and zonal modes, respectively, in *Kurt et al. (2004)*. In the following relations the Rayleigh number R^s for stationary convection is expressed as a function of the input parameters, E_z, Λ and α, and the horizontal wave numbers, l and m, therefore $R^s = R^s(E_z, \Lambda, \alpha; l, m)$. We introduce also, for a clear comparison of the isotropic and anisotropic cases, the auxiliary variable[6]

$$l_\alpha = \frac{K_\alpha^2}{K^2} = \frac{A_\alpha}{A} = \frac{1 + \alpha\tilde{a}}{1 + \tilde{a}} = l_\alpha(\tilde{a}, \alpha). \tag{20}$$

Using tedious algebra, we derive from (17) at $\lambda = 0$

$$R^s = \pi\, l_\alpha \frac{K^3}{a^2}\left\{C_\alpha + \frac{\tilde{l}}{C_\alpha}\right\} = \pi^2\, l_\alpha \frac{A^{3/2}}{\tilde{a}}\left\{C_\alpha + \frac{\tilde{l}}{C_\alpha}\right\}, \tag{21}$$

$$C_\alpha = \frac{E_z}{\pi}\, l_\alpha K^3 + \frac{\Lambda m^2}{\pi K} = \pi^2 E_z l_\alpha A^{3/2} + \frac{\Lambda.\widetilde{m}}{A^{1/2}} \quad \text{with} \quad A = 1 + \tilde{a}. \tag{22}$$

The formulas (21, 22) correspond to (18ab) in *Kurt et al. (2004)* and to (5.3, 5.4) in *Eltayeb (1972)* and one can see that after some algebra they are coincident ($1_\alpha = 1$ and $C_\alpha = C$ for $\alpha = 1$).

Minimizing R^s with respect to the variables $\tilde{a}$ and C_α (and not to $\tilde{l}$ and $\widetilde{m}$ in a complicated way) we get at $\varepsilon = \pi^2 E_z/\Lambda$ two equations

$$(\tilde{a} + \varepsilon\, l_\alpha A^2)A = \Lambda^2(\widetilde{m} + \varepsilon\, l_\alpha A^2)^2 \qquad \text{and}$$

$$\widetilde{m} = \frac{[1 - \alpha\tilde{a}(1 + 2\tilde{a})]\,[\tilde{a} + A(1 + \alpha\tilde{a})\varepsilon]}{1 - \alpha\tilde{a}^2} \tag{23}$$

for the two unknowns $\tilde{m}$ and $\tilde{a}$, determining the critical horizontal wave vector (l_c, m_c), but only for SO modes. Consequently the critical Rayleigh number for SO modes,

$$R_c^{SO} = \pi^2 l_\alpha \frac{A_c^{3/2}}{\tilde{a}_c}\left\{2C_c - \frac{A_c^{1/2}}{\Lambda}\right\} = R_c^{SO}(\tilde{a}_c, C_c), \tag{24}$$

---

[6] Denoted 1_α, because $1_\alpha = 1$ in the isotropic case $\alpha = 1$.

is added to the relations for the critical wave numbers (23), where $l_\alpha(\tilde{a})$ and $C_\alpha(\tilde{a})$ are expressed for $\tilde{a}_c$ ($C_c = C_\alpha(\tilde{a}_c)$).

Numerical computations show that, at constant E_z, the SO modes gradually rotate from being perpendicular to the magnetic field to being increasingly parallel to it with increasing Elsasser number, Λ, and that at a certain value of Λ, i.e. $\Lambda = \Lambda^{SO/P}$, the tilt angle equals $0°$, at which they switch to P modes. That is why it is interesting to derive the value $E_z^{SO/P}$ of the Ekman number, $E_z = E_z(\Lambda, \alpha)$, at which transition of SO into P modes occurs. The critical horizontal wave number $a_c = \pi \tilde{a}_c^{1/2}$ for P modes with $\widetilde{m} = 0$ is given from the second of (23) by

$$\tilde{a}_c = 1/4 \left[(1 + 8/\alpha)^{1/2} - 1 \right] = \tilde{a}_c^P(\alpha) \equiv a_0, \qquad (25)$$

and is independent of the Ekman number E_z. The matching of the SO and P modes can be achieved by substituting (25) into the first of (23) with $\widetilde{m} = 0$. This defines the boundary $E_z = E_z(\Lambda, \alpha) \equiv E_z^{SO/P}$ between the two modes in the form

$$E_z = \frac{\sqrt{c_1} + \sqrt{c_1 + c_2 \Lambda^2}}{\pi^2 \Lambda}, \quad \text{where} \quad c_1 = \frac{1}{4(1 + \alpha a_0)^2}, \quad c_2 = \frac{4c_1 a_0}{1 + a_0} \qquad (26)$$

are functions only of the parameter α and for $\alpha = 1$ they are the simple numbers $c_1 = 1/9$ and $c_2 = 4/27$. In (26), $\Lambda \equiv \Lambda^{SO/P}$, i.e. Λ as well as E_z are the transition values $\Lambda^{SO/P}$ and $E_z^{SO/P}$, respectively. The parallel steady modes were identified by *Eltayeb (1972)* in his equation (5.15), but in his double limit of large Taylor ($= E^{-2}$) and Hartmann ($= (\Lambda/E)^{1/2}$) numbers[7] these modes cannot be preferred.

We can express analytically only continuous SC/SO transition, not discontinuous one. We obtain, by comparison of the critical horizontal wave numbers for the SC and SO modes, a parametric representation of the function $\Lambda = \Lambda(E_z, \alpha)$ where $\Lambda \equiv \Lambda^{SC/SO}$, $E \equiv E_z^{SC/SO}$, and, for the sake of clarity, we perform it only for the isotropic case, $\alpha = 1$, when $E_z = E$. We have

$$E = \pi^{-2} \frac{\tilde{a}}{1 + \tilde{a}} \sqrt{\frac{\tilde{a}}{(1 - 2\tilde{a})(1 - \tilde{a}^2)}} \quad \text{and} \quad \Lambda = \sqrt{\frac{(1 - 2\tilde{a})(1 + \tilde{a})}{(1 - \tilde{a})\tilde{a}}}, \qquad (27)$$

---

[7] In *Eltayeb (1972, 1975)* there were good reasons for using the same dimensionless numbers as in *Chandrasekhar (1961)*.

where $\tilde{a} = a_c^2/\pi^2$. Thus the "normalized" square of the critical horizontal wave number is in the role of the parameter. We get, by direct comparison of this parametric representation and the numerically computed line, that the boundary, from which the parametric representation characterizes the continuous SC/SO transition is $\Lambda = \Lambda_s \doteq 2.35$ and the corresponding $E_s \doteq 0.0075$. For $\Lambda \leq \Lambda_s$ and $E \geq E_s$ the tilt angle of the rolls passes continuously from $90°$ for the SC modes to $90°$ for the SO modes, while for $\Lambda \geq \Lambda_s$ and $E < E_s$ it jumps from $90°$ to some other angle less than $90°$. Thus, the SC/SO transition is not continuous for $\Lambda > \Lambda_s$ and $E < E_s$ and (27) cannot be used. Hence, for $\Lambda \leq \Lambda_s$ and $E \geq E_s$, the relation (27) corresponds to the dashed line representing the boundary between the SC and SO modes on the ΛE_z regime diagram in Figure 3a. For investigated anisotropy with $\alpha = O(1)$, Λ_s as well as E_s are monotonous functions of α.

Finally, we compare the stationary convection quantitative data in *Kurt et al. (2004)* and our results. We consider the roughly estimated values of quantities[8] in Fig. 3b in *Kurt et al. (2004)* as sufficiently consistent with the information in the ΛE_z regime diagram in the Fig. 3a.

4.2. Non-stationary modes

We introduce the following auxiliary substitutions (by the analogous $\mathcal{V}$ case in *Roberts and Jones (2000)*)

$$\lambda = i\sigma, \quad y = \frac{\sigma}{K^2}, \quad y_\alpha = \frac{\sigma}{K_\alpha^2}, \quad \phi = \frac{\Lambda m^2}{\pi K}, \quad x = \frac{R a^2 E_z}{\pi^2} \quad \text{and}$$

$$c_\alpha = \frac{E_z K K_\alpha^2}{\pi}. \tag{28}$$

In the isotropic case it is valid to set $y_\alpha = y$, $K_\alpha = K$ and $c_\alpha = c$. After additional algebraic operations, we get equation (17) in the form

$$q_z x(1 + iy)\{c_\alpha(1 + iy) + \phi\} =$$
$$= (q_z + iy_\alpha)c_\alpha \left\{ [c_\alpha(1 + iy) + \phi]^2 + \tilde{l}(1 + iy)^2 \right\}. \tag{29}$$

At the same time, the new variables present in it, which are proportional to the physical quantities like the Rayleigh number, Ekman number or the

---

[8] The regime τQ diagram in the Fig. 3b in *Kurt et al. (2004)* is for the quantities $\tau = E^{-1}$ and $Q = \Lambda E^{-1}$.

frequency, are expressed by means of relations (28). For example, the variables x and x/c_α are both proportional to the Rayleigh number, R, but the latter is also independent of the Ekman number E_z.

4.3. Non-stationary modes; limit $E_z \to 0$

In the large ν limit, $\nu \gg \kappa \sim \eta$, the neglect of E_z (7) can be related to the high angular velocity, Ω_0, which is the case for the Earth's rotation. Furthermore, due to the stress free boundaries the boundary layer phenomena for $E_z = O(1)$ are excluded from our model. Thus, the mathematical simplicity due to infinite Prandtl numbers, ν/κ and ν/η, and $E_z \ll 1$ is sufficiently heuristic for the Earth's core conditions.

The limit $E_z \to 0$ ($c_\alpha \to 0$) leads to the following (29) simplification

$$\frac{q_z x}{c_\alpha}(1 + iy)\phi = (q_z + iy_\alpha)[\phi^2 + \tilde{l}(1 - y^2 + 2iy)]. \tag{30}$$

Using the condition $\Im m(x) = 0$ and the inverse transformations $y = \sigma/K^2$ and $y_\alpha = \sigma/K_\alpha^2$ we obtain an important relation for the frequency σ,

$$\sigma^2 = K^4 \left[\frac{q_\alpha - 1}{q_\alpha + 1} \frac{\phi^2}{\tilde{l}} - 1 \right] \quad \text{with} \quad q_\alpha = q_z l_\alpha, \tag{31}$$

where l_α is introduced in (20). The relation (31) shows, that in the inviscid case, $c_\alpha = 0$ ($E_z = 0$), the OC modes do not exist, because for $\tilde{l} = 0$ the frequency is infinitely large, which, naturally, cannot occur. It is valid for all α, for the isotropic and anisotropic cases.

After some algebra we obtain

$$\frac{x^o}{c_\alpha} = \frac{2}{q_\alpha} \left\{ \psi + \frac{\tilde{l}}{\psi} \right\} \quad \text{with} \quad \psi = \frac{\phi}{q_\alpha + 1}, \tag{32}$$

which allows us to express the formula for the Rayleigh number as

$$R^o = \pi \frac{K K_\alpha^2}{a^2} \left(\frac{x^o}{c_\alpha} \right) = \frac{2\pi}{q_z} \frac{K^3}{a^2} \left\{ \psi + \frac{\tilde{l}}{\psi} \right\}. \tag{33}$$

Note that the dependence of R^o on the anisotropy is hidden only in ψ, hence in q_α by (20) and the 2nds of (31, 32).

5. Numerical results

Focusing attention on the influence of anisotropic diffusion coefficients on the onset of convection we try to accomplish two important comparisons. First, to distinguish the isotropic case (*Brestenský and Šoltis, 2014*) and compare it with the two types of SA anisotropy, Sa and So (in the $\mathcal{H}$ case So and BM anisotropies are coincident). Second, to compare the $\mathcal{H}$ and $\mathcal{V}$ cases (*Šoltis and Brestenský, 2010*) from the point of view of the SA anisotropy only, because in the BM one in the $\mathcal{V}$ case the broken horizontal isotropy causes complexities for presentation of results.

5.1. Approaches to the solution

The numerical search for the critical Rayleigh number R_c is performed in the same way as in the $\mathcal{V}$ case and described in *Šoltis and Brestenský (2010)*. The analogous "critical" effective Rayleigh number, $R_{ce} = R_c/\alpha$, is simply derived from the relation (8) between the Rayleigh numbers, R and R_{eff}, corresponding to their critical and "critical" numbers, R_c and R_{ce}, respectively. The quotation marks in "critical" are used, because R_c determines R_{ce}. Henceforth, we will often use the critical effective Rayleigh number for the R_{ce}, despite the fact that R_{ce} is the result of minimization R and not R_{eff}.

It is standard procedure that, at this stage of the solution the results are obtained numerically, and the important ones selected from them are confirmed at appropriate limits with asymptotic methods (see section 4). In the analytically performed minimization, frequently two independent variables are derived from the basic independent variables, e.g. from the horizontal components of the wave number, while one of them is a function not only of the wave number but also of the selected input parameters, e.g. the Ekman or/and Elsasser numbers. This enables us to minimize much more effectively and transparently.

5.2. Different effects of anisotropy on the stationary and nonstationary convection

Likewise, in the $\mathcal{V}$ case (*Šoltis and Brestenský, 2010*), we investigated how rolls with different orientations are preferred in the space of parameters, Λ

and E_z, and how this ΛE_z regime diagram, distribution of the preference regions of individually oriented rolls, is influenced by anisotropy of the diffusion coefficients. The influence of anisotropy manifests itself in the change of SC/SO and SO/P boundaries between the regions. The *So* anisotropy ($\alpha > 1$) reduces the preference region of oblique SO rolls and, vice versa, the *Sa* anisotropy ($\alpha < 1$) extends this region (Fig. 3). From the physical point of view this can be interpreted as a weakening or strengthening of the effects of the Lorentz and Coriolis forces, where the qualitative effects depend not only on anisotropy itself but also on the regime of the convection. The *So* anisotropy with $\alpha > 1$ weakens the effect of the Lorentz force and strengthens the effect of the Coriolis force in the regime close to the SC/SO boundary (in the *Sa* case, $\alpha < 1$, this weakening and strengthening is opposite; the influence of the *So* and *Sa* anisotropies is qualitatively reversed in the regime close to the SO/P boundary.)

The investigation of the influence of anisotropy on the onset (the critical Rayleigh number) and the form (critical wave numbers) of steady convec-
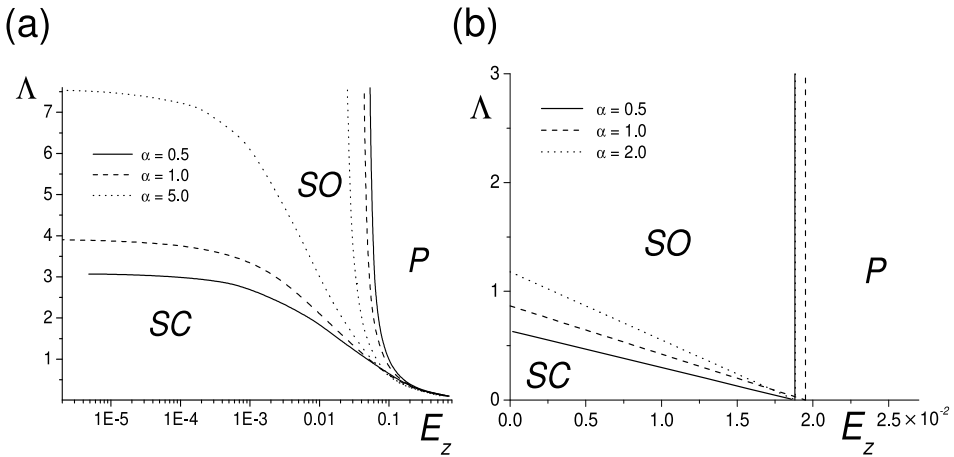

Fig. 3. Stationary convection; the ΛE_z diagrams for the isotropic case $\alpha = 1$ and for two anisotropic cases, *So* and *Sa*, in the $\mathcal{H}$ case (a) and $\mathcal{V}$ case (b). The SC, SO and P rolls are preferred in the correspondingly labeled regions. In (a) the asymptotes of the SC/SO and SO/P lines in the isotropic case are the horizontal line, $\Lambda = 4$, and vertical line, $E2\sqrt{3}/(9\pi^2) \doteq 0.039000$. The main qualitative difference between ΛE_z regime diagrams in the $\mathcal{H}$ and $\mathcal{V}$ case is the nonexistence of the "tail" in the $\mathcal{V}$ case in which the SC/SO and SO/P boundaries are straight lines and not curves.

290

tion shows that the R_c is an increasing function of α, but $R_{ce} = R_c/\alpha$ is a decreasing function of α (see Fig. 4 and Table 2.). However, if the Ekman number is small enough (say $E_z = 3 \cdot 10^{-7}$ here), the R_c of the SC modes is independent of anisotropy in the $\mathcal{H}$ case (Fig. 4a). Unfortunately, we cannot conclude whether the anisotropy (Sa or So) stabilizes or destabilizes the layer. The critical horizontal wave number a_c is a decreasing function of α, which means, that the So anisotropy increases the horizontal sizes of the stationary convection rolls and the Sa anisotropy decreases them (Fig. 5). The change of preference between the SC and SO modes is accompanied with a sharp jump in values of the horizontal wave number, so the change of preference from the SC to SO modes does not occur continuously with the increase of the Elsasser number, Λ, like in the $\mathcal{V}$ case.
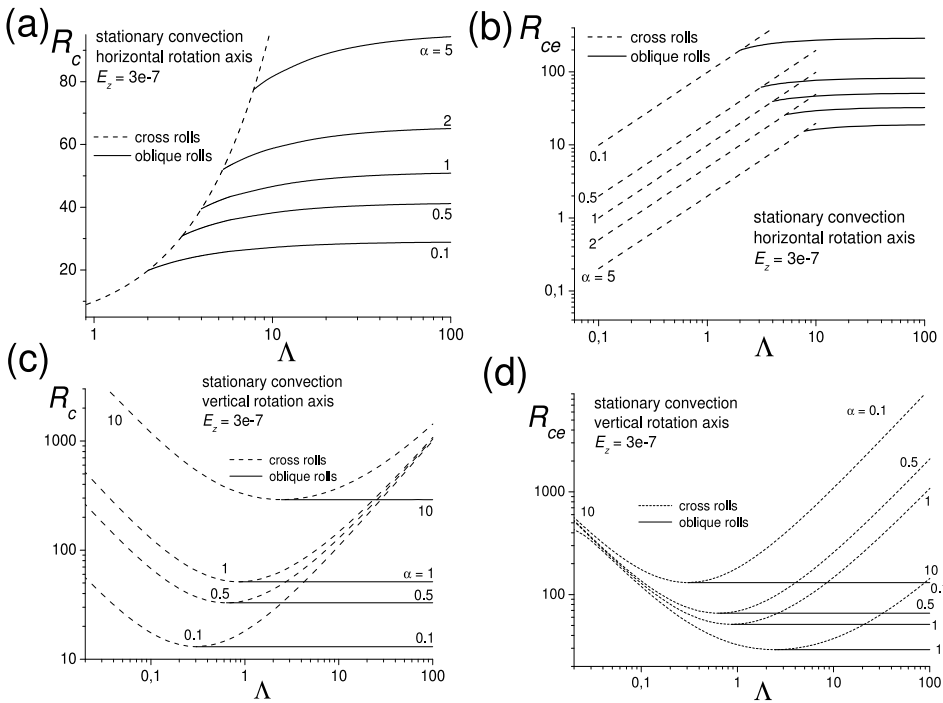

Fig. 4. Effect of SA anisotropy on steady convection. Dependences of the critical Rayleigh numbers, R_c and $R_{ce} = R_c/\alpha$, on the Elsasser number Λ at the Ekman number $E_z = 3 \cdot 10^{-7}$ in the $\mathcal{H}$ case (ab) and in the $\mathcal{V}$ case (cd); cross and oblique rolls = SC and SO modes.
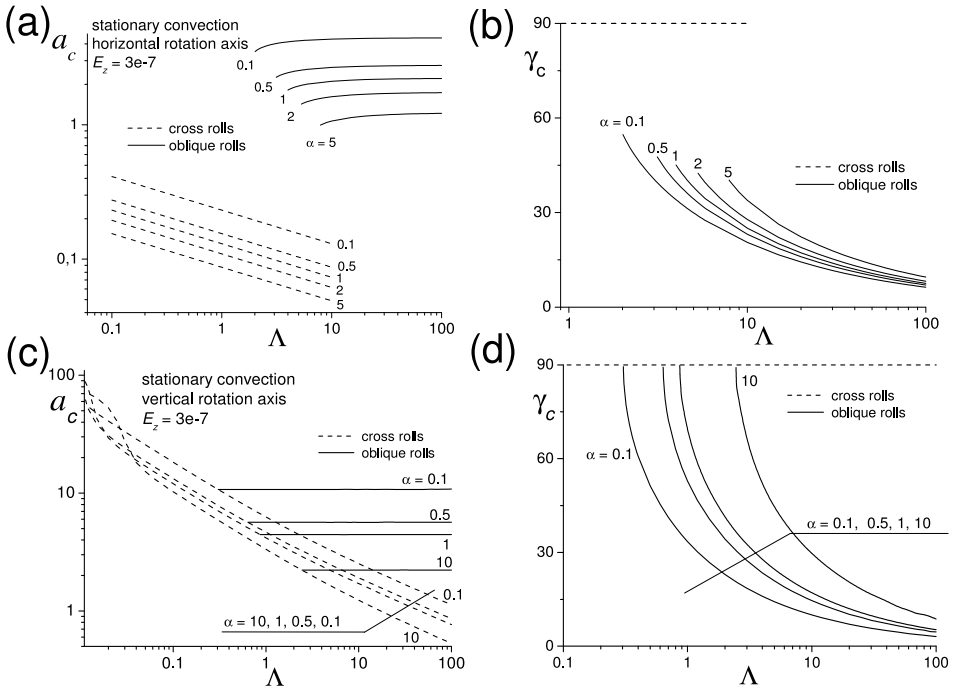
Fig. 5. Influence of anisotropy on the stationary convection. Dependences of the critical horizontal wave number a_c and the critical angle γ_c on the Elsasser number Λ at the constant Ekman number $E_z = 3 \cdot 10^{-7}$ in the $\mathcal{H}$ case (ab) and in the $\mathcal{V}$ case (cd). The a_c is decreasing and γ_c increasing function of α. It means, that if the diffusion in the horizontal directions is enhanced ($\alpha > 1$), the horizontal dimension of the rolls is increased and the rolls are more inclined to the axis of rotation and vice versa.

When examining the non-stationary convection, our attention was concentrated on a simpler two dimensional Λq_z regime diagram, dividing the space of parameters, Λ and q_z, into 5 preference regions, SC, SO, OC, OO and OC'; see Section 4. The OC' modes, the non-stationary convective rolls almost parallel to the rotation axis, revealed by *Eltayeb (1975)*, do exist only in the $\mathcal{H}$ case. Likewise OC, the OC' modes do not exist in the inviscid case, $E = 0$. The SC/OC boundaries for $q_z \gtrsim 2$ are in very good agreement with the formula $\Lambda \sim [\pi^2 E_z/(q_z - 1)][(a_0 + 1)^2/a_0]$ asymptotically determined for $q_z \gg 1$, $\Lambda \ll \pi^2 E_z$ and $\alpha = O(1)$; for $a_0 = a_0(\alpha)$ see (25). For $\Lambda \to \infty$ the SO/OO boundaries are asymptotically determined by

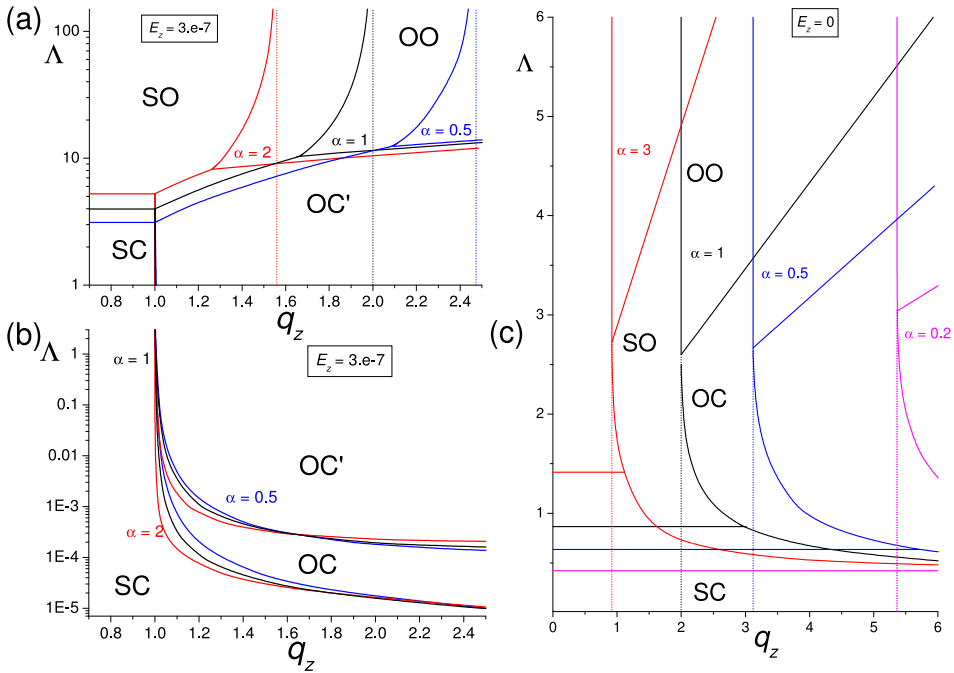Fig. 6. The Λq_z regime diagram for stationary and non-stationary convection for two anisotropic, Sa and So, and isotropic cases for $E_z = 3 \cdot 10^{-7}$ and $E_z = 0$ in $\mathcal{H}$ and $\mathcal{V}$ cases, respectively. Contrary to the $\mathcal{V}$ case in (c) the regime diagram in the $\mathcal{H}$ case is divided into two parts (a) and (b), namely for larger $\Lambda \geq O(1)$ and smaller $\Lambda \leq O(1)$. The OC' modes are only in $\mathcal{H}$ case. The three (red, black and blue) groups of lines, representing the boundaries between preference regions, are related to the three values of anisotropy parameter, $\alpha = 0.5$, 1 and 2.

$q_z = [3/(1 + \alpha a_0)][3a_0/(1 + a_0)]^{1/2}$, identical with the verticals[9] in Fig. 6a.

   Since anisotropy influences more or less all critical numbers describing convection (see Table 2) the conditions of matching of modes are also affected by anisotropy. Therefore, anisotropy influences significantly the position of the lines forming the boundaries between these 5 regions in the Λq_z regime diagram. The system of lines (except of boundaries related to the OC modes) is shifted towards the smaller or higher values of Λ and q_z

---

[9] In the $\mathcal{V}$ case the SO/OO preference boundaries for $\Lambda \to \infty$ are marked in Fig. 6c, and are asymptotically determined by $q_z = 3\sqrt{3}\, 2_\alpha (2_\alpha + 1)^{1/2} (\alpha 2_\alpha + 1)^{-1}, 2_\alpha = [1 + (8 + \alpha)^{1/2}]/(2\,\alpha)$; $q_z = 2$ and $2_\alpha = 2$ for $\alpha = 1$.

Table 2. Qualitative effect of the SA anisotropy on the steady and non-stationary modes of convection in the $\mathcal{H}$ and $\mathcal{V}$ cases. Three symbols, $\uparrow, \downarrow$ and $-$, mean that the critical numbers $R_c, R_{ce}, a_c, \gamma_c$ and σ_c are increasing, decreasing and independent of the anisotropy parameter, α, respectively. In the $\mathcal{H}$ case, the effects of the So and BM anisotropies on the arising convection are the same.

	$\mathcal{H}$ case steady conv.	$\mathcal{H}$ case non-stationary conv.	$\mathcal{V}$ case steady conv.	$\mathcal{V}$ case non-stationary conv.
R_c	$\uparrow$	$\downarrow$ (OO, OC′) $-$ (OC)	$\uparrow$	$-$ (OO) $\downarrow$ (OC)
R_{ce}	$\downarrow$	$\downarrow$	$\downarrow$	$\downarrow$
a_c	$\downarrow$	$\uparrow$ (OO, OC′) $-$ (OC)	$\downarrow$	$-$ (OO) $\uparrow$ (OC)
γ_c	$\uparrow$	$\uparrow$	$\uparrow$	$\uparrow$
σ_c		$\uparrow$ (OO, OC′) $-$ (OC)		$\uparrow$

depending on the value of α, where, however, the overall frame of the lines is not changed by anisotropy.

The results for the critical numbers are richer for nonstationary modes than for stationary convection and much richer if we compare the results for $\mathcal{H}$ and $\mathcal{V}$ cases. Accepting the unique situation in the $\mathcal{H}$ case that the OC′ modes, de facto special OO modes, also represent the OC modes for $\Lambda \leq O(1)$, then the change of preference from OC′ to OO modes is analogous to the change of preference from stationary SC to SO modes. Thus, there is a sharp jump in the critical values of the horizontal wave number and frequency, which is not analogous to the $\mathcal{V}$ case in which the change of preference from OC to OO modes is related to the continuous change of the critical numbers at the transitional value of Λ. Furthermore, the OC and OO rolls have roughly twice as large horizontal sizes and their critical frequency σ_c is much greater in the $\mathcal{H}$ case compared with the $\mathcal{V}$ case. In the $\mathcal{H}$ case there is no constraint on the nonstationary convection with respect to the value of the Elsasser number Λ, but in the $\mathcal{V}$ case the nonstationary convection does not exist for Λ smaller than some onset Λ, which is a function of the anisotropy parameter α. We can see it as the sharp left end of

the dashed lines in Figure 7d which correspond to the drop of frequences to the zero value in Figure 7f.

The study of anisotropy effects on the onset of convection (Figs. 4, 5 and 7, 8) reveals a peculiar difference between oblique stationary and non-stationary modes. The same anisotropy has a completely opposite influence on the critical numbers (Rayleigh, R_c and R_{ce}, and horizontal wave numbers a_c) of SO stationary modes in comparison with OO non-stationary modes. The So (or the BM) anisotropy with horizontal diffusivities greater than the vertical ones, $\alpha > 1$, decreases R_c and R_{ce} as well as the horizontal size of the OO rolls of the non-stationary convection. Further, it increases R_c, but decreases R_{ce} and a_c of the stationary convection (SO). Thus we can conclude that the So anisotropy destabilizes the layer with respect to non-stationary OO modes, but we cannot say the same in the case of stationary SO modes. The Sa anisotropy with $\alpha < 1$, has the qualitatively opposite effect, with opposite monotonicity of critical numbers (changing decrease to increase and vice versa), than the So anisotropy. The similarly opposite effects of So and Sa anisotropies are valid also for the SC modes and partly for the OC modes. The R_c and a_c of the OC modes are independent of anisotropy (see Table 2).

5.3. Rayleigh numbers

The effect of anisotropy on the onset of convection should be determined with the definition of the Rayleigh number, which gives a true picture of its physical mechanism. We used (*Šoltis and Brestenský, 2010*) the vertical thermal diffusivity κ_{zz} in the mathematical definition (8) of the Rayleigh number $R = g\alpha_T \Delta T d / 2\Omega_0 \kappa_{zz}$, despite the fact that the horizontal thermal diffusivity, $\kappa_{xx} = \kappa_{yy} = \alpha \kappa_{zz}$, is important for the convection weakening the vertical temperature gradient (see e.g. *Manneville, 2004*). The vertical thermal diffusivity κ_{zz} apears in the definition (8) of the first Rayleigh number R naturally because of the choice of the scale of the dimensionless temperature perturbation ϑ in (6). However, the temperature difference between upwelling and downwelling fluids is significant at the onset of convection and therefore the horizontal diffusivity, $\kappa_{xx} = \alpha \kappa_{zz}$, can be also important in the case of anisotropy. Thus, the physically relevant Rayleigh number, labeled R_{eff}, is defined by R in the second formula of (8), $R_{eff} = R/\alpha$.
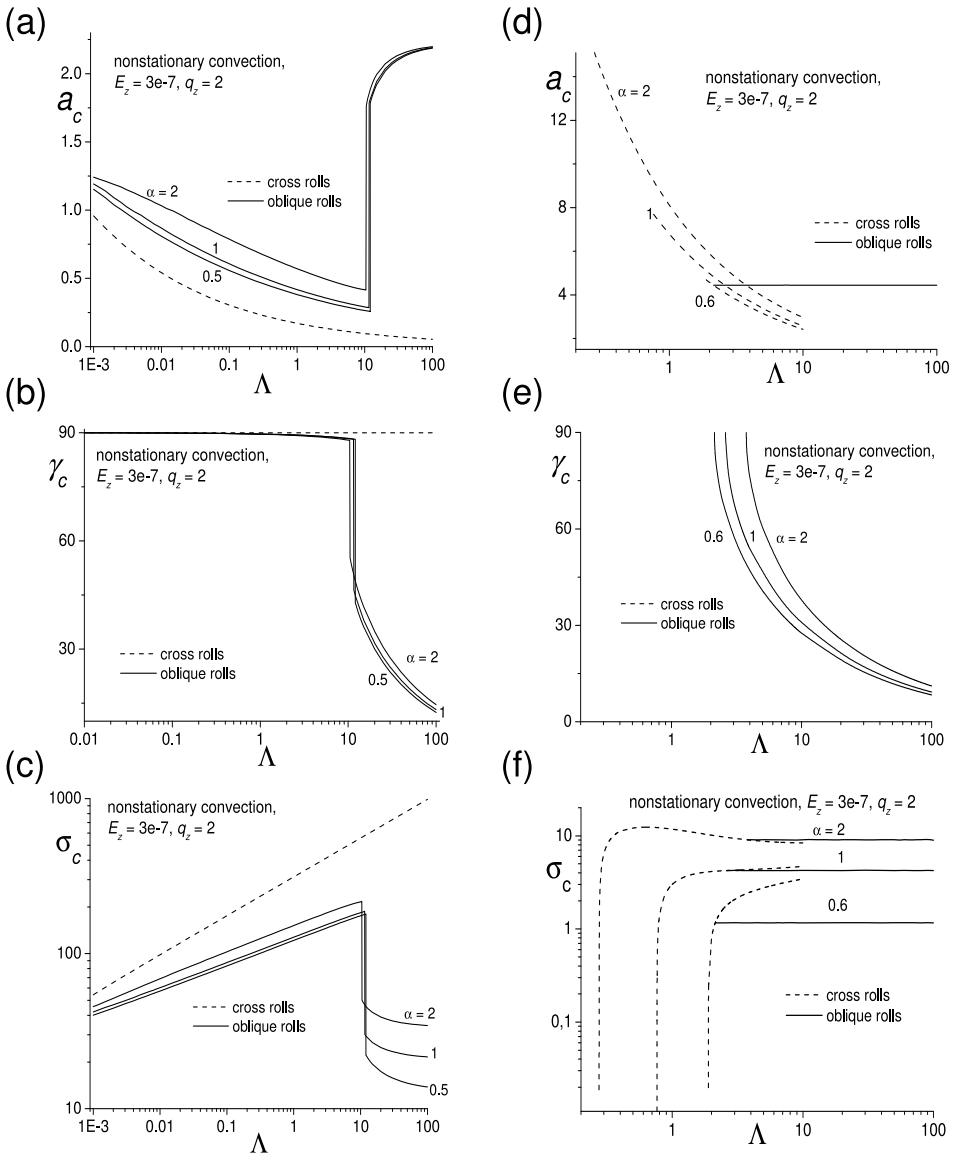
Fig. 7. Effect of anisotropy on non–stationary convection. Dependences of the critical numbers – the horizontal wave number, a_c, angle γ_c and frequency, σ_c – on the Elsasser number Λ for the Ekman $E_z = 3 \cdot 10^{-7}$ and the Roberts number $q_z = 2$ in the $\mathcal{H}$ case (abc) and $\mathcal{V}$ case (def); cross and oblique rolls = OC and OO modes, and the left parts of the solid lines correspond to the OC′ modes in (abc).
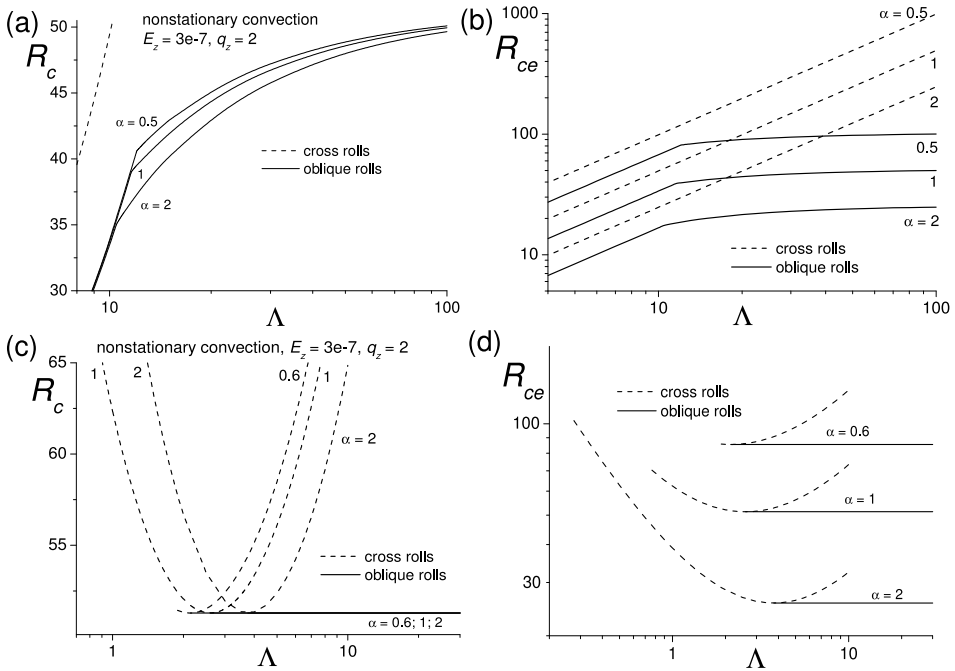
Fig. 8. Comparison of the critical Rayleigh number R_c and the "critical" effective Rayleigh number $R_{ce} = R_c/\alpha$ as a function of the Elsasser number Λ for the nonstationary convection in the $\mathcal{H}$ case (ab) and in the $\mathcal{V}$ case (cd); cross and oblique rolls = OC and OO modes, and the left and steeper parts of the solid lines correspond to the OC′ modes in (ab).

Since in this paper the minimization and the search for the critical Rayleigh number was done for R and not R_{eff}, all regime diagrams and critical horizontal wave numbers and frequences related to the "critical" R_{eff}, labeled R_{ce} (see subsection 5.1.), are the same as for R_c, despite the fact that R_{ce} and R_c are different due to the obvious relation $R_{ce} = R_c/\alpha$.

The motivation for such a definition of the Rayleigh number in the anisotropic case is the apparent disagreement of the results in the $\mathcal{V}$ case (Šoltis and Brestenský, 2010) and the results in Ivers and Phillips (2007–2012) and possibly in Donald and Roberts (2004), besides the correct physical understanding of convection. Ivers and Phillips (2007–2012) noticed this discrepancy between Ivers and Phillips (2007–2012) and Šoltis and Brestenský (2010), solving the problem of the effect of the anisotropic ther-

mal diffusivity on rotating convection with no magnetic field in spherical geometry, in which they considered enhanced (or diminished) diffusion in the z direction of the rotation axis to other directions of cylindrical coordinates, i.e. s and azimuthal φ; see also Tables 1 and 2. Their anisotropy, which is roughly analogous to our SA anisotropy, has the opposite effect on the onset of convection (the critical Rayleigh number) as it is in our $\mathcal{V}$ case. It means that if our anisotropy "facilitates" the onset of convection (decreases the critical Rayleigh number R_c), the anisotropy in *Ivers and Phillips (2007–2012)* "inhibits" the convection (increases the R_c). The quotation marks in "facilitates" and "inhibits" present the authors' opinion that in the anisotropic cases there could be another physically more convenient definition of the Rayleigh number than is R or R_{eff}. This opinion is similarly related to other models, e.g. in *Ivers and Phillips (2007–2012)* or *Donald and Roberts (2004)*; see also the Table 1. Some results of *Donald and Roberts (2004)* can be compared with our results from some point of view which can only qualitatively indicate the similarity/dissimilarity of the anisotropy effects on the Rayleigh numbers in *Donald and Roberts (2004)* and *Šoltis and Brestenský (2010)*. *Donald and Roberts (2004)* showed, that introducing anisotropy, $\beta > 0$ (analogous to our $\alpha < 1$; $\beta = (1-\alpha)/(1+\alpha)$) makes the convection stronger and $\beta < 0$ ($\alpha > 1$) weakens the convection. However, their Rayleigh number is much higher then the critical Rayleigh number and their developed convection is far beyond the onset. Therefore we do not have direct information about the influence of anisotropy on the critical Rayleigh number in their model.

In the case $\mathcal{H}$ investigated here, there is agreement for the nonstationary convection with results in *Ivers and Phillips (2007–2012)*, but the effect of anisotropy on the onset of the stationary convection is still qualitatively opposite in comparison with *Ivers and Phillips (2007–2012)* (different monotonicity of $R_c(\alpha)$). By introduction of the effective Rayleigh number R_{eff} (maybe physically more convenient than the previously defined Rayleigh number R) the agreement is achieved also in stationary convection, which can be seen in Figures 4b and 8b (and in Table 2 in section 6, too) as equal ordering of the curves R_{ce}, "critical" R_{eff}, as functions of the anisotropy parameter α. Similarly, as in our $\mathcal{V}$ case, the qualitatively equal effect of anisotropy on the onset of convection, as in the case studied by *Ivers and Phillips (2007–2012)*, and possibly the dynamo problem (*Donald and*

Roberts, 2004) by Donald and Roberts, was confirmed by introduction of R_{eff}. The most convenient definition of the Rayleigh number in the cases with anisotropic diffusivities is yet an open problem, but there is a promising approach by *Ivers and Phillips (2012)* to solve it.

6 Conclusions

The influence of anisotropy of thermal diffusivity and viscosity, determined by the anisotropy parameter α defined in the last of (7), on the model of rotating magnetoconvection in the horizontal plane layer was investigated using a linear stability analysis. The layer rotates about the horizontal axis in the x-direction and is permeated with a homogeneous magnetic field in the horizontal y-direction. The layer is heated from below and cooled from above and a uniform temperature gradient is sustained.

We investigated instabilities, i.e. stationary convection and/or non-stationary convection, in the form of horizontal rolls (in the same way as in the $\mathcal{V}$ case (*Šoltis and Brestenský, 2010*)). Depending on input parameters, the modes SO, SC, P, OO, OC′ and OC can occur; see section 4. The typical values of input parameters are not only geophysically relevant ones, i.e. $E_z \ll 1$, $\Lambda \leq O(10)$ and $q_z \leq O(1)$, but they also involve values comparable to values frequently used in geodynamo simulations. Due to the considered limits for diffusion coefficients, $\nu \gg \kappa \sim \eta$, attention was mainly focused on the MAC dynamics. The orientation of the rolls with respect to the magnetic field and rotation axis is related to the Coriolis and Lorentz forces. Results of their competition (but also of the Archimedean force) are well expressed for all investigated modes of convection by two types of regime diagrams, ΛE_z and Λq_z, and dependences of critical numbers on Λ.

A comparison of two models, the cases $\mathcal{H}$ and $\mathcal{V}$, with different, horizontal and vertical, orientations of the rotation axis, respectively, was done for various $\alpha \neq 1$ of the SA anisotropy and for isotropic diffusivities with $\alpha = 1$. There are many differences in convection between the cases $\mathcal{H}$ and $\mathcal{V}$. The important difference is that a certain type of mode occurs only in the $\mathcal{H}$ case and not in the $\mathcal{V}$ case, for all investigated α. If, in the $\mathcal{H}$ case, the Coriolis force dominates the Lorentz force ($\Lambda \ll 1$), the convection is two dimensional (with respect to the axis of rotation) and independent of rotation. With increasing Λ, the Lorentz force becomes important for all α, but

it has only a stabilizing effect, because there is no local decrease of $R_c(\Lambda)$ at $\Lambda = O(1)$. Thus, the rotation alone (with no or very week magnetic field) about the horizontal axis does not inhibit convection, but it suppresses the inhibiting effect of the magnetic field on convection at $\Lambda = O(1)$ more effectively than in the case of vertical rotation axis; see *Brestenský and Šoltis (2014), Eltayeb (1972, 1975), Eltayeb and Rahman (2013)* for $\alpha = 1$.

The rotation axis in the vertical direction, $\mathcal{V}$ case, is always perpendicular to the axis of the rolls, which has a significantly different effect in comparison with the $\mathcal{H}$ case with a horizontal axis of rotation. The effect of the SA anisotropy on the stationary convection is qualitatively very similar in both $\mathcal{V}$ and $\mathcal{H}$ cases, for instance the monotonicities of critical numbers dependences on the anisotropy parameter α are the same; see Table 2. The main difference is between ΛE_z regime diagrams (Fig. 3) with the nonexistence of the "tail" in the $\mathcal{V}$ case in which the SC/SO and SO/P boundaries are straight lines and not curves.

More significant differences between the $\mathcal{H}$ and $\mathcal{V}$ cases are in the nonstationary case. In the $\mathcal{H}$ case there is no constraint on the nonstationary convection with respect to the value of the Elsasser number Λ, but in the $\mathcal{V}$ case the nonstationary convection does not exist for Λ smaller than some onset Λ, which is a function of α.

In the $\mathcal{V}$ case and in other rotating magnetoconvection models the Lorentz force weakens the Proudman-Taylor constraint at $\Lambda = O(1)$, but in the $\mathcal{H}$ case the cross modes are independent of rotation and therefore the rotational constraint in the usual way (like in the $\mathcal{V}$ case) does not exist. For all α at $q_z = O(1)$ the OC and OC′ modes are preferred to the oblique OO modes even for strong magnetic fields with $\Lambda \geq O(10)$. Thus the Lorentz force has to be much stronger than the Coriolis force to cause the rolls to become inclined to the basic magnetic field. This is very similar to the axially-aligned motions, nearly 2D motions with respect to the axis of rotation in spherical geometry, which persist even for strong magnetic fields, $\Lambda = O(10)$ (see e.g. *Gubbins and Herrero-Bervera, 2007*), but dissimilar to the $\mathcal{V}$ case where OC modes are preferred to OO modes only for smaller $\Lambda \leq O(1)$.

The OC modes in the $\mathcal{H}$ case are parallel to the rotation axis and are not influenced by anisotropy, because the critical numbers, R_c, a_c and σ_c, are not functions of α. In the $\mathcal{V}$ case, R_c and a_c of the OO (and not OC) modes

are independent of α. The effect of anisotropy on the OO modes manifests itself in the inclination γ_c of their rolls and contrary to OC modes, in the dependence of the critical frequency σ_c on α; see Table 2. Thus, the qualitatively opposite effect of SA anisotropy on the stationary and non-stationary convection is valid also in the $\mathcal{V}$ case, where R_c for OC modes is a decreasing function of α, opposite to the stationary case.

In the $\mathcal{H}$ case the monotonic dependence of R_c on α for some modes is different from the spherical case (*Ivers and Phillips, 2007–2012*). An analogous difference (but for other modes) was also found for the $\mathcal{V}$ case. "The critical" R_{ce} of the introduced effective Rayleigh number $R_{e\!f\!f}$ (8) has the same monotonicity on α in both $\mathcal{H}$ and $\mathcal{V}$ cases (see Table 2) and like the critical Rayleigh number in *Ivers and Phillips (2007–2012)*. Therefore, in the plane geometry of our $\mathcal{V}$ and $\mathcal{H}$ cases $R_{e\!f\!f}$ based on the thermal diffusivity components in the directions perpendicular to gravity could be a more convenient choice than an R based on the component in the direction parallel to gravity. We can only indicate that in the spherical geometry, the choice of the Rayleigh number is much more complex in a rotating fluid with anisotropic diffusion coefficients.

References

Aurnou J., 2007: Planetary core dynamics and convective heat transfer scaling. Geophys. Astrophys. Fluid Dyn., **101**, 5–6, 327-345.

Braginsky S. I., Meytlis V. P., 1990: Local turbulence in the Earth's core. Geophys. Astrophys. Fluid Dynam., **55**, 2, 71–87.

Brestenský J., Šoltis T., Ševčík S., 2005: Linear Rotating Magnetoconvection with anisotropic diffusive coefficients. In: Proceedings of the Riga Pamir conference, Fundamental and Applied MHD 1, 101–104.

Brestenský J., Šoltis T., 2014: Hydromagnetic instabilities in the plane layer rotating about horizontal rotation axis. Geophys. Astrophys. Fluid Dynam. (submitted).

Chandrasekhar S., 1961: Hydrodynamic and hydromagnetic stability. Clarendon Press, Oxford.

Cushman-Roisin B., 1994: Introduction to Geophysical Fluid Dynamics. Prentice Hall.

Donald J. T., Roberts P. H., 2004: The effect of Anisotropic heat transport in the Earth's core on the Geodynamo. Geophys. Astrophys. Fluid Dynam., **98**, 5, 367–384.

Eltayeb I. A., 1972: Hydromagnetic convection in a rapidly rotating fluid layer. Proc. R. Soc. Lond. A, **326**, 229–254.

Eltayeb I. A., 1975: Overstable hydromagnetic convection in a rapidly rotating fluid layer. J. Fluid Mech., **71**, 161–179.

Eltayeb I. A., Rahman M. M, 2013: Model III: Benard convection in the presence of horizontal magnetic field and rotation. Phys. Earth Planet. Inter., **221**, 38–59.

Fearn D. R., Roberts P. H., 2007: The geodynamo, Chapter 4. In: Dormy E., Soward A. M. Mathematical Aspects of Natural Dynamos. Taylor and Francis.

Gailitis A. K., Lielausis O. A., Platacis E., Gerbeth G., Stefani F., 2002: Colloquium: Laboratory experiments on hydromagnetic dynamos. Reviews of Modern Physics, **74**, 973-990.

Gubbins D., Herrero-Bervera E., 2007: Encyclopedia of Geomagnetism and Paleomagnetism. Springer.

Ivers D. J., Phillips C. D., 2007–2012: Personal communication.

Ivers D. J., Phillips C. D., 2012: Anisotropic Turbulent Thermal Diffusion and Thermal Convection in a Rapidly Rotating Fluid Sphere. Phys. Earth Planet. Inter., **190–191**, 1–9.

Jones C. A., Roberts P. H., 2000: The Onset of Magnetoconvection at Large Prandtl Number in a Rotating Layer II. Small Magnetic Diffusion. Geophys. Astrophys. Fluid Dynam., **93**, 173–226.

Kurt E., Busse F. H., Pesch W., 2004: Hydromagnetic convection in a rotating annulus with an azimuthal magnetic field. Theoret. Comput. Fluid Dynamics, **18**, 2–4, 251–263.

Manneville P., 2004: Instabilities, Chaos and Turbulence; An Introduction to Nonlinear Dynamics and Complex Systems. Imperial College Press, London.

Matsushima M., Nakajama T., Roberts P. H., 1999: The anisotropy of local turbulence in the Earth's core. Earth Planet Space, **51**, 4, 277–286.

Phillips C. G., Ivers D. J, 2003: Strong Field Anisotropic Diffusion Models for the Earth's core. Phys. Earth Planet. Inter., **140**, 1–3, 13–28.

Roberts P. H., Jones C. A., 2000: The Onset of Magnetoconvection at Large Prandtl Number in a Rotating Layer I. Finite Magnetic Diffusion. Geophys. Astrophys. Fluid Dynam., **92**, 3–4, 289–325.

Schubert G., 2007: Treatise on Geophysics, Volume 5 – Geomagnetism, ed. Kono M., Volume 8 – Core Dynamics, ed. Olson P., Elsevier.

Šimkanin J., Brestenský J., Ševčík S., 2003: Problem of the rotating magnetoconvection in variously stratified fluid layer revisited. Studia Geophys. Geod., **47**, 4, 827–845.

Šoltis T., Brestenský J., 2010: Rotating magnetoconvection with anisotropic diffusivities in the Earth's core. Phys. Earth Planet. Inter., **178**, 1–2, 27–38.

Šoltis T., 2010: The influence of anisotropic diffusivities on hydromagnetic instabilities in the Earth's core conditions. PhD Thesis, Fac. of Maths, Physics & Informatics, Comenius University, Bratislava (in Slovak).